Tetrathiaoxa Macrocycles with Dibenzo-subunits: A Search for New Tl(I)- and Ag(I)-Selective Ionophores

Ki-Min Park[a]; Yoon Hee Lee[a]; Yongri Jin[a]; Joobeom Seo[a]; IL Yoon[a]; Sang Cheol Lee[b]; Sung Bae Park[b]; Myoung-Seon Gong[c]; Moo Lyong Seo[a]; Shim Sung Lee[a]

[a] Department of Chemistry and Research Institute of Natural Sciences, Gyeongsang National University, Chinju, S. Korea [b] Department of Chemistry, Inje University, Kimhae, S. Korea [c] Department of Chemistry, Dankook University, Chungnam, S. Korea

PLEASE SCROLL DOWN FOR ARTICLE

Taylor & Francis
Taylor & Francis Group

Tetrathiaoxa Macrocycles with Dibenzo-subunits: A Search for New Tl(I)- and Ag(I)-Selective Ionophores

KI-MIN PARK[a], YOON HEE LEE[a], YONGRI JIN[a], JOOBEOM SEO[a], IL YOON[a], SANG CHEOL LEE[b], SUNG BAE PARK[b,]*, MYOUNG-SEON GONG[c], MOO LYONG SEO[a] and SHIM SUNG LEE[a,]*

[a]*Department of Chemistry and Research Institute of Natural Sciences, Gyeongsang National University, Chinju 660-701, S. Korea;* [b]*Department of Chemistry, Inje University, Kimhae 621-749, S. Korea;* [c]*Department of Chemistry, Dankook University, Cheonan, Chungnam 330-714, S. Korea*

Novel S_4O_n mixed donor macrocycles (1, $n = 1$; 2, $n = 2$) were synthesized by the coupling reactions of corresponding dichlorides with dithiols under high dilution conditions. Synthesis and crystal structures of Tl^+ and Ag^+ complexes, $[Tl(2)^+$ and $Ag(2)^+]$, with macrocycle 2 are described. The electrode based on macrocycle 2 showed excellent potentiometric sensing ability for Tl^+ and Ag^+ ions. This remarkable sensing of the proposed electrode can be understood in terms of the synergy effect of a soft–soft acid–base interaction and π-coordination, especially for the Tl^+ ion, which was observed from the crystal structure of the corresponding complex.

Keywords: Macrocyclic complex; Crystallography; Thallium; Ion-selective electrodes; Silver

INTRODUCTION

Thiaoxa macrocycles have received considerable attention due to not only to their role as a connection between homoleptic crown ethers and thia macrocycles [1–3], but also to their ability to discriminate between metal ions during separation and electrochemical detection [4–6]. In fact, some S_2O_n ($n = 1, 2$) mixed donor macrocycles incorporating monobenzo subunits have been reported as excellent receptors in Ag^+-selective electrodes [5,6]. Thus, increasing interest has been directed toward the design and synthesis of new thiaoxa macrocyclic ionophores for the development of new receptors for soft metal ions in ion-selective electrodes [7–12].

π-Coordination between soft metal ions, such as Ag^+, Cu^+ and Tl^+ ions and aromatic molecules represents an important class of intermolecular forces in supramolecular chemistry and has frequently been proposed as an alternative source for the improvement of selectivity in the development of metal ion receptors [13–16]. Based on this consideration, so far, synergic Ag^+–π interactions in macrocyclic systems, such as calix[4]arenes [17] and double-armed diaza-18-crown-6 derivatives [18], have proved applicable in the development of sensing materials. Calix[4]arene derivatives [19,20] also have been applied successfully for Tl^+ ionophores, taking advantage of the π-coordination.

As mentioned, soft metal–arene interactions are relatively weak but selective. Our interest in soft metal complexation and detection [3,6,18,20–22] has led us to search for and synthesize new macrocycles containing both a multi-binding sulfur donor and an aromatic subunit simultaneously. Thus, the synthesis and coordination properties, including sensing systems for the tetrathiaoxa-dibenzo macrocycles (**1** and **2** in Scheme 1), have become our target. Herein, as an application of these receptors, we report the synthesis of the target ligands and their complexes, together with their crystal structures and their usage in soft-metal sensing.

EXPERIMENTAL

Materials and Physical Techniques

Diacid **3** was obtained by the reaction of thiosalicylic acid with dibromoethane [23]. The reduction of diacid **3** with $LiAlH_4$ gave 2,2'-(ethylenedithio)bis(benzyl alcohol) **4** [23]. All reagents were of analytical grade. Melting points are uncorrected. Infrared spectra were

*Corresponding authors. E-mail: sslee@nongae.gsnu.ac.kr; chempsb@ijnc.inje.ac.kr
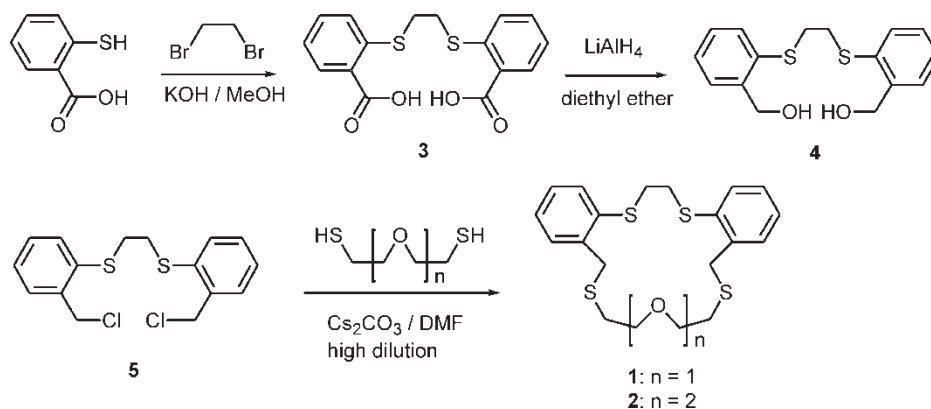
SCHEME 1

measured on a Mattson Genesis Series FT-IR spectrophotometer. ^{1}H and ^{13}C NMR spectra were recorded on a Bruker DRX-500 spectrometer operating at 500 and 125.7 MHz, respectively. Microanalyses were done by Elemental Analysen Systeme Vario EL and mass spectra were obtained on a Kratos Profile HV-3 spectrometer at the Korea Basic Science Institute, Pusan Branch. Thin-layer chromatography was carried out on plates coated with Merck Silica gel UV-254. For flash column chromatography, Merck Silica gel 60 (No. 9385, 230–400 mesh) was used.

Synthesis of Dichloride 5

To a stirred, cooled ($-14°C$) suspension of compound **4** (2.3 g, 7.5 mmol) in dichloromethane (150 ml) was added thionyl chloride (3.54 g, 30 mol) in one portion. The reaction mixture was maintained at this temperature for 15 min, then allowed to warm gradually to room temperature; stirring was continued overnight. Ethanol (95%, 5 ml) was added carefully, and the reaction mixture stirred at room temperature for a further 2 h. The solvent was evaporated off to yield a light pink solid. Water (100 ml) was added, and the mixture was extracted with dichloromethane (3 × 50 ml). The organic phase was dried over anhydrous sodium sulfate and filtered, and the solvent was removed to yield a white solid **5** (1.342 g) in 52% yield. This product was purified by recrystallization from 95% ethanol to yield colorless needles. Compound **5**, colorless needles, 500 MHz ^{1}H NMR (CDCl$_3$): δ 3.18 (s, SCH$_2$, 4H), 4.84 (s, ArCH$_2$, 4H), 7.27–7.51 (m, aromatic, 8H). 125 MHz ^{13}C NMR (CDCl$_3$): δ 33.1 (SCH$_2$), 45.1 (ArCH$_2$), 127.3, 129.6, 130.4, 131.1, 135.6, 137.8 (aromatic).

Synthesis of Macrocycle 1

Caesium carbonate (3.78 g, 11.6 mmol) was dissolved in DMF (1000 ml) in a 3-l round-bottomed flask.

The appropriate dithiol (0.81 g, 5.8 mmol) and dichloride **5** (2.01 g, 5.8 mmol) were dissolved in DMF (30 ml) and 50 ml of this solution were taken up into a glass syringe. Under a nitrogen atmosphere, the contents of the syringe were added dropwise at a constant rate (0.6 ml h^{-1}) to a DMF solution of caesium carbonate by means of a syringe pump at 45–50°C for 50 h. The mixture was kept for a further 10 h. After being cooled to room temperature the reaction mixture was filtered and evaporated. Water (100 ml) was added, and the mixture was extracted with dichloromethane (3 × 50 ml). The organic phase was dried over anhydrous sodium sulfate and filtered, and the solvent was removed to give a yellow oil. Flash column chromatography (SiO$_2$; *n*-hexane–ethyl acetate 8:2) afforded the product as a white solid (0.080 g, 0.2 mmol) in 3.5% yield. Macrocycle **1**, white solid, mp 104–106°C; 500 MHz ^{1}H NMR (CDCl$_3$): δ 2.74 (t, $J = 6.45$ Hz, 4H, OCH$_2$CH_2S), 3.18 (s, 4H, ArCH$_2$S), 3.66 (t, $J = 6.50$ Hz, 4H, SCH$_2$CH$_2$S), 4.04 (s, 4H, OCH_2CH$_2$S), 7.18–7.40 (m, 8H, aromatic); 125 MHz ^{13}C NMR (CDCl$_3$): δ 32.32, 35.08, 35.25, 71.38, 127.80, 128.13, 130.74, 132.14, 134.87, 140.57; IR (KBr disk) 1265.01, 1412.48, 1465.13, 2880.12 cm^{-1}; mass spectrum *m/z* 408 (M, 26%), 285 (9), 271 (10), 259 (8), 212 (15), 211 (8.5), 181 (16), 153 (100), 149 (32), 122 (37), 121 (37). Anal. Calcd. for C$_{20}$H$_{24}$OS$_4$: C, 58.78; H, 5.92; S, 31.39, Found: C, 59.17; H, 5.71; S, 31.55.

Synthesis of Macrocycle 2

The synthetic procedure is almost the same as for macrocycle **1** except for the use of 2,2'-(ethylenedioxy)bis(ethanedithiol) as the dithiol. Flash column chromatography (SiO$_2$; *n*-hexane–ethyl acetate 7:3) afforded the product as a white solid in 7.8% yield. Macrocycle **2**, white solid, mp 108–110°C; 500 MHz ^{1}H NMR (CDCl$_3$): δ 2.72 (t, $J = 6.45$ Hz, 4H, OCH$_2$CH_2S), 3.13 (s, 4H, OCH$_2$CH$_2$O), 3.60 (s, 4H, SCH$_2$CH$_2$S), 3.68 (t, $J = 6.45$ Hz, 4H, OCH_2CH$_2$S), 4.02 (s, 4H, ArCH$_2$S), 7.17–7.40 (m, 8H, aromatic);

TABLE I   Crystal data and refinement parameters

Compound	5	1	[Ag(2)]$_2$(ClO$_4$)$_2$	[Tl(2)]PF$_6$
Formula	C$_{16}$H$_{16}$Cl$_2$S$_2$	C$_{20}$H$_{24}$OS$_4$	C$_{22}$H$_{28}$AgClO$_6$S$_4$	C$_{22}$H$_{28}$F$_6$O$_2$PS$_4$Tl
M	343.31	408.63	660.00	802.02
Crystal system	Monoclinic	Monoclinic	Triclinic	Monoclinic
a (Å)	12.4361(16)	7.8632(6)	13.0168(6)	12.0774(8)
b (Å)	8.5318(11)	26.195(2)	13.8973(7)	10.2313(7)
c (Å)	7.7392(10)	4.8913(4)	15.2227(7)	22.8400(17)
α (°)	90	90	69.1230(10)	90
β (°)	98.898(2)	96.133(2)	87.5570(10)	101.0740(10)
γ (°)	90	90	89.6620(10)	90
V (Å^3)	811.26(18)	1001.75(14)	2570.5(2)	2769.7(3)
D$_c$ (g cm^{-3})	1.405	1.355	1.705	1.923
μ (mm^{-1})	0.644	0.480	1.250	6.251
Space group	P2$_1$/c	Cm	P$\bar{1}$	P2$_1$/n
Z	2	2	4	4
F(000)	356	432	1344	1560
Dimensions (mm)	0.18 × 0.30 × 0.40	0.10 × 0.35 × 0.40	0.20 × 0.25 × 0.40	0.20 × 0.30 × 0.40
T (K)	298(2)	298(2)	298(2)	298(2)
2θ$_{max}$ (°)	56.50	56.58	56.66	56.74
No. measured	5085	3319	16685	17637
No. unique	1952	1603	11773	6581
Parameters	92	124	655	335
R1 [I > 2σ(I)]	0.0640	0.0366	0.0479	0.0511
wR$_2$ (all data)	0.2392	0.1090	0.1346	0.1530

125 MHz ^{13}C NMR (CDCl$_3$): δ 31.99, 34.96, 34.73, 70.68, 71.41, 127.42, 127.73, 130.35, 134.44, 140.34; IR (KBr disk) 1211.62, 1347.82, 1412.54, 1467.27, 2877.99 cm^{-1}; mass spectrum m/z 452 (M, 40%); 424 (3), 363 (2), 329 (7), 303 (10), 272 (8), 271 (14), 243 (17), 242 (8), 212 (10), 181 (19), 180 (8), 153 (100), 149 (30), 122 (32),121 (35), 91 (15), 78 (11), 77 (10), 61(8); Anal. Calcd. for C$_{22}$H$_{28}$O$_2$S$_4$: C, 58.37; H, 6.23; S, 28.33, Found: C, 58.23; H, 6.17; S, 28.53.

X-ray Crystallography

All data were collected on a Bruker SMART diffractometer equipped with a graphite mono-chromated Mo-Kα (λ = 0.71073 Å) radiation source and a CCD detector; 45 frames of two-dimensional diffraction images were collected and processed to obtain the cell parameters and orientation matrix. Two-dimensional diffraction images were collected, each of which was measured for 30 s. The frame data were processed to give structure factors using the program SAINT [24]. The structure was solved by a direct methods and refined by full-matrix least squares against F^2, for all data using SHELXTL software [24]. Absorption corrections were based on multiple and symmetry-equivalent reflections in the data sets using the SADABS program [25] for the silver complexes. All non-H atoms were refined with anisotropic displacement parameters. A summary of the crystallographic data is given in Table I. X-ray crystallographic files in CIF format have been deposited with the Cambridge Crystallographic Data Centre (CCDC reference numbers 182363, 182364, 182365, 184823).

Ion-selective Electrodes

The ionophore, PVC, and plasticizer (diisodecyl adipate) were used in the weight ratio 6.0, 31.7, and 62.3 [26]. After allowing the membranes to cure, 5.5 mm diameter disks were cut out and placed in Phillips electrode bodies (ISE-561, Glasblaserei Moller, Zurich). As an internal filling solution, 1 mM AgNO$_3$ was used for all electrodes. Cell potentials were measured at ambient temperature (18°C). The potentiometric cell used was as follows: Ag/AgCl(s)/4M KCl saturated with AgCl/Tris buffer/sample solution/ion-selective membrane/1 mM AgNO$_3$/AgCl(s)/Ag. The ion-selective and Ag/AgCl reference electrodes were connected through a high impedance amplifier to an IBM AT-type computer equipped with an A/D converter. The sampling rate was adjusted to 1 Hz. Almost Nernstian slopes are observed in 0.05 M Tris-nitric acid buffer, pH 9.0. The time required to reach 90% equilibrium mV values was less than 2 s. In terms of lifetime of the PVC membrane electrodes, more than 1 month of response stability was observed. This apparatus was used to determine the selectivity of each membrane toward Ag$^+$ ion over other cations in the static mode. Selectivity coefficients, $k^{pot}_{Ag/x}$, were obtained by using the separate solution method at 1 mM cation concentration [27].

RESULTS AND DISCUSSION

Synthesis of Macrocycles 1 and 2

The reduction of diacid 3 with LiAlH$_4$ led to the dialcohol 4. Chlorination of 4 with SOCl$_2$ yielded

the dichloride **5** as a key precursor. For the final cyclization of precursor **5** with the dithiols, conditions employing caesium carbonate in DMF under high dilution conditions [28] were successful in giving the macrocycles **1** and **2** (Scheme 1).

Crystal Structures of Dichloride 5 and Macrocycle 1

Colorless crystals of dichloride **5** that proved suitable for X-ray crystallography were obtained by recrystallization from ethanol. In the crystal, precursor **5** possesses a C_2 axis and the two Cl atoms are oriented away from each other. The torsion angle between the two phenyl S atoms (S1—C1—C1A—S1A), which has the value 180°, is fully in the *trans* arrangement (Fig. 1(a)). It is known that 1,4-interactions between heteroatoms (E = O, N or S) in the —E—CH$_2$—CH$_2$—E— bond depend on whether E is a first- or second-row element [29–31]. For example, O and N heteroatoms stabilize the *gauche* conformation because of the dispersion forces between the hetero E atoms. In contrast, for E = S, the larger size of the atoms causes greater repulsion between electrons, which disfavors *gauche* conformations. The present rules readily apply to the structure of **5** shown in Fig. 1(a). The observed lower yields of cyclizations for **1** and **2** are not unusual and may be attributed to the conformation of the precursor **5** which shows the two Cl atoms oriented away from each other due to the repulsive interaction between the two phenyl S atoms in the solid state.

Colorless crystals of macrocycle **1** for X-ray crystallography were grown by slow evaporation from dichloromethane–*n*-hexane (v/v 0.45:0.55). However the preparation of single crystals for macrocycle **2** was not available. The crystal structure of macrocycle **1** indicates that it exists in a non-folded configuration (Fig. 1(b)). It has a mirror plane which passes through O1 and the mid-point of C1—C1′A. The molecule is partially disordered with C1—C1′A and C1′—C1A units occupying two positions. Two

exo-dentate benzyl sulfur donors tend to be separated as far apart as possible; they lie, together with the centroid of aromatic rings, at the corners of a pseudo-rectangular plane (ca. 7.8 × 4.0 Å). The aliphatic segment between the two benzyl S atoms (S2—C9—C10—O1—C10A—C9A—S2A) spans *trans* arrangements with torsion angles of 176.4–176.7°. The dihedral angle between the two aromatic systems is 29.1(1)°.

Crystal Structures of the Complexes

Reaction of silver perchlorate with one mole equivalent of **2** in methanol yielded a colorless solid. Single crystals suitable for crystallography were obtained from an acetonitrile solution by slow evaporation. The results of an X-ray study are shown in Fig. 2, with structural parameters listed in Table II. The unit cell of the silver complex of **2** contains a pair of unusual crystallographcally independent molecules A and B. In both complexes, each macrocycle encircles one silver atom in an *endo* manner. A remarkable conformational difference of the two molecules is the geometry of the coordination sphere around the metal centers.

In molecule A, the coordination geometry of the Ag1 atom is distorted tetrahedral with the four coordination sites being occupied by the sulfur atoms of **2**. The macrocyclic ligand **2** adopts an arrangement that removes the O donors from the coordination sphere. The silver to benzyl sulfur bonds [Ag1—S3A 2.521(1), Ag1—S2A 2.530(1) Å] are marginally shorter than the mean (2.675 Å, with standard deviation of 0.015 Å) of such bonds taken from the X-ray literature [32,33], but the silver to phenyl sulfur bonds [Ag1—S1A 2.689(1), Ag1—S4A 2.741(1) Å] are slightly longer than average values. The distortion from regular tetrahedral symmetry is reflected by the considerable variation of bond lengths and angles about the metal center. A detailed inspection of the ORTEP diagram for
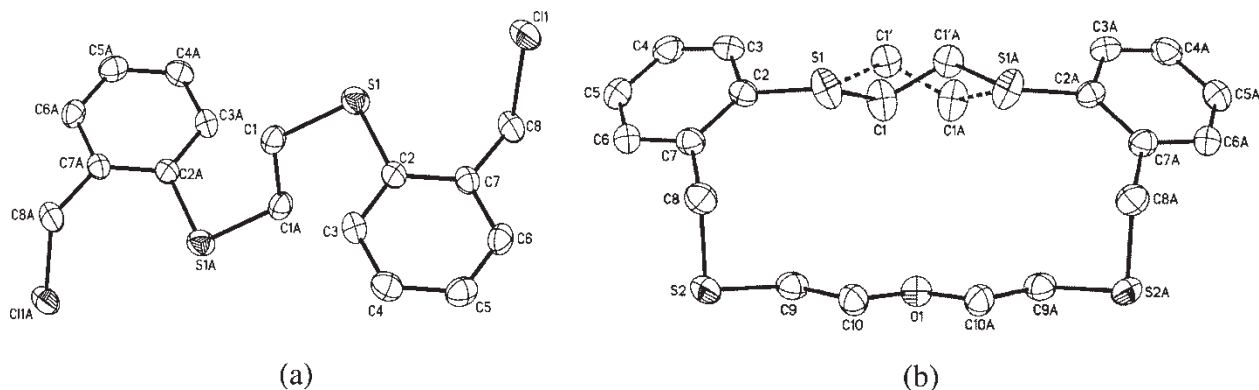

FIGURE 1   Crystal structures of (a) **5** and (b) **1** with atom-numbering scheme. Displacement ellipsoids are drawn at the 30% probability level. H atoms and anions have been omitted for clarity.
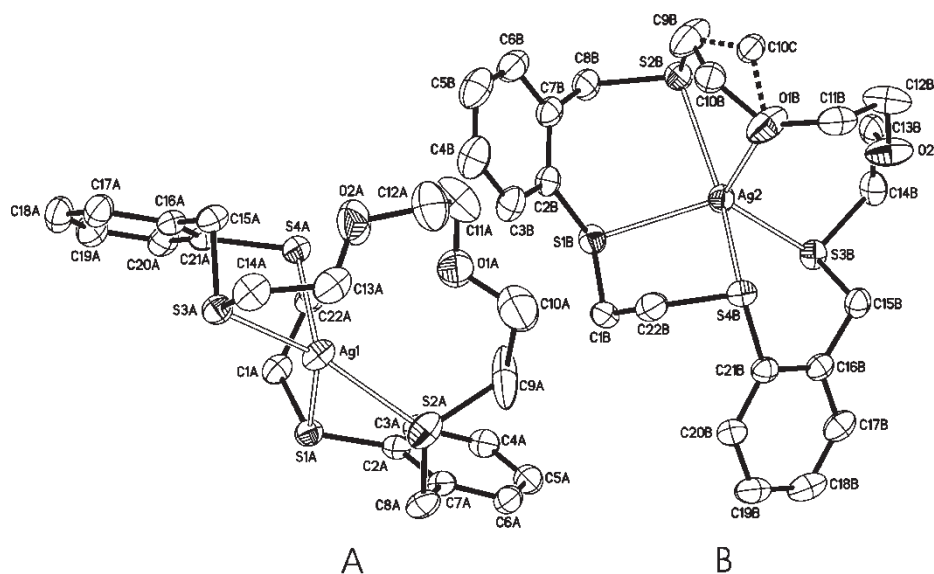
FIGURE 2 Crystal structures of two forms (A and B) of $[Ag(2)]_2^{2+}$ with atom-numbering scheme. Displacement ellipsoids are drawn at the 30% probability level. H atoms and anions have been omitted for clarity.

the molecule A reveals that the structure of the macrocycle is folded and also highly twisted. The additional weak interaction between the silver and oxygen atom [Ag1···O1A 3.075(4) Å] produces a marked distortion from regular tetrahedral geometry: the S1A—Ag1—S4A angle is decreased to 81.34(3)° and the S2A—Ag1—S4A is increased to 135.70(4)° due to the presence of the Ag1···O1 interaction. The silver to benzyl sulfur bonds [Ag2—S3B 2.545(1), Ag2—S2B 2.568(1) Å] are slightly longer than those of molecule A, but still marginally shorter than the mean values of the literature [32,33]. Meanwhile, the silver to phenyl sulfur bonds [Ag2—S1B 2.671(1), Ag2—S4B 2.725(1) Å] are slightly shorter than those of molecule A and are comparable to average values. The Ag2—O1B bond

[2.729(4) Å] appears somewhat elongated although it falls within the range 2.4–2.8 Å reported for similar bonds in other Ag^+ complexes [33,34]. The remaining O2B atom is outside bonding distance to the metal center.

Equimolar amounts of $TlNO_3$ and NH_4PF_6 were added to a solution of 2 in acetonitrile–methanol (v/v 1:1). The colorless complex crystallized on slow evaporation of the resulting solution. X-ray analysis revealed that the [Tl(2)]PF_6 has the *endo*-dentate conformation shown in Fig. 3. The structural parameters are listed in Table III. A metal ion coordinating to a macrocyclic ligand is normally expected to sit in the cavity of the ring or to be located not far from the mean plane of the donor atoms of the macrocycle. According to Fig. 3,

TABLE II Selected bond lengths (Å), bond angles and torsion angles (°) of $[Ag(2)]_2(ClO_4)_2$

Ag1—S3A	2.5213(11)	Ag1—S2A	2.5298(12)
Ag1—S1A	2.6891(11)	Ag1—S4A	2.7407(11)
Ag2—S3B	2.5451(11)	Ag2—S2B	2.5678(12)
Ag2—S1B	2.6705(11)	Ag2—S4B	2.7249(10)
Ag2—O1B	2.729(4)		
S3A—Ag1—S2A	126.78(4)	S3A—Ag1—S1A	128.24(4)
S2A—Ag1—S1A	88.91(4)	S3A—Ag1—S4A	91.46(3)
S2A—Ag1—S4A	135.70(4)	S1A—Ag1—S4A	81.34(3)
S3B—Ag2—S2B	128.59(4)	S3B—Ag2—S1B	126.11(4)
S2B—Ag2—S1B	88.51(4)	S3B—Ag2—S4B	89.28(3)
S2B—Ag2—S4B	136.19(4)	S1B—Ag2—S4B	83.40(3)
S1A—C1A—C22A—S4A	64.0(4)	S3A—C14A—C13A—O2A	66.8(5)
O2A—C12A—C11A—O1A	65.2(7)	O1A—C10A—C9A—S2A	61.6(2)
S1B—C1B—C22B—S4B	69.1(4)	S3B—C14B—C13B—O2B	62.3(5)
O2B—C12B—C11B—O1B	65.9(6)	O1B—C10B—C9B—S2B	46(1)
O1B—C10C—C9B—S2B	44(1)		

Front view   Side view
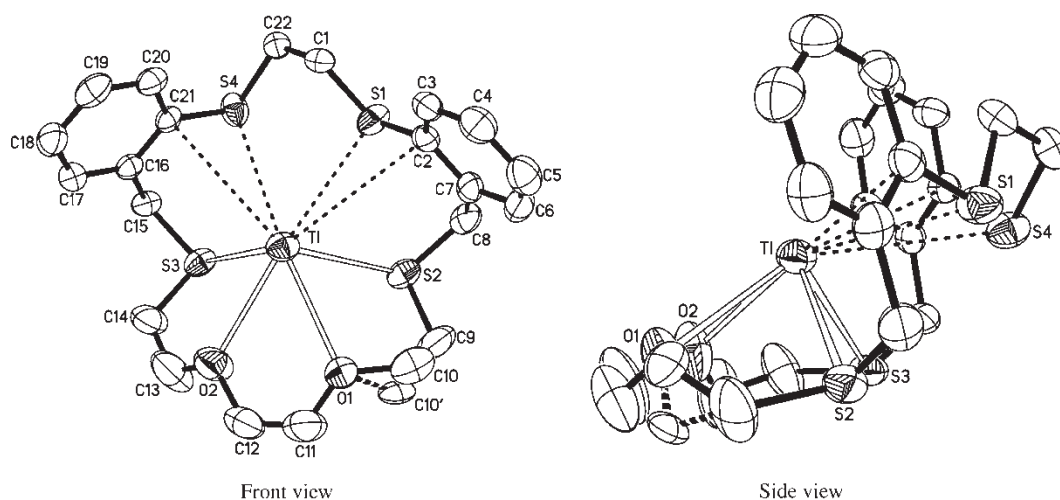
FIGURE 3   Crystal structure of [Tl(**2**)]$^+$ with atom-numbering scheme. Displacement ellipsoids are drawn at the 30% probability level. H atoms and anions have been omitted for clarity.

however, the macrocycle **2** adopts a three dimensional baseball-glove-like conformation and the thallium ion is as far as 1.815(3) Å above the mean S_2O_2 donor plane (O1, O2, S2, S3; average deviation; 0.0067 Å) of the macrocycle. It is quite surprising to see the Tl$^+$ floating above the macrocyclic plane. Therefore, the Tl$^+$ coordination cannot be described simply in terms of a regular polyhedron. The Tl$^+$ center involves four-coordination with two Tl—S bonds [Tl—S2 3.161(2), Tl—S3 3.223(2) Å] and two Tl—O bonds [Tl—O1 2.864(6), Tl—O2 2.867(7) Å] lying within sum of the van der Waals radii, 3.8 and 3.5 Å [35], respectively. The two other S atoms are outside bonding distance to the metal center [Tl⋯S1 3.469(3), Tl⋯S4 3.855(2) Å] [36] so they can be considered as short interactions. The bond angles between adjacent Tl—O or Tl—S bonds range from 57.0(2) to 103.3(1)° consistent with the unusual quadrupodal structure (Fig. 3).

More interestingly, interactions between the thallium atom and aromatic π-system [16,37,38] were observed [Tl⋯C2(arene), 3.699(6); Tl⋯C21(arene), 3.828(6) Å]. Each thallium to carbon interaction is at the long end of the range of literature values (3.36–3.88 Å) [16,37,38]. It is conceivable that a combination of Tl⋯S and Tl⋯arene interactions would lead to the dislocation of the Tl$^+$ from the mean

plane of S_2O_2 donor set and subsequently promote the formation of the baseball-glove-like conformation as shown in Fig. 3. Upon complexation, the molecular folding of **2** is so exceptional that this may reflect, at least in part, evidence of the high selectivity for Tl$^+$ in the solid state as well as in solution. Thus, such findings of inclusive complexation, including π-coordination in the solid state structures, were enough to motivate us to study the carrier-based membrane electrodes. Our repeated efforts to obtain the crystal structures of Ag$^+$ or Tl$^+$ complexes of **1** were not successful.

Ion-selective Electrodes

By employing the macrocycle **2** in conjunction with potentiometric ion sensors [4,5], it was possible to observe Ag$^+$ and Tl$^+$ responses. In a pH response study, the pH was evaluated by titrating 0.05 M phosphoric acid with 0.1 M sodium hydroxide. The pH response was relatively low (typically less than 15 mV per decade). To minimize the presence of protons (or hydrated water), however, 0.05 M Tris buffer (pH 9.0) was used throughout the present study [9]. Approximately 6.0 wt% of **2** in PVC matrix yielded electrodes with near-Nernstian responses (54–55 mV/decade) over a wide range of Ag$^+$ and

TABLE III   Selected bond lengths (Å), bond angles and torsion angles (°) of [Tl(**2**)]PF$_6$

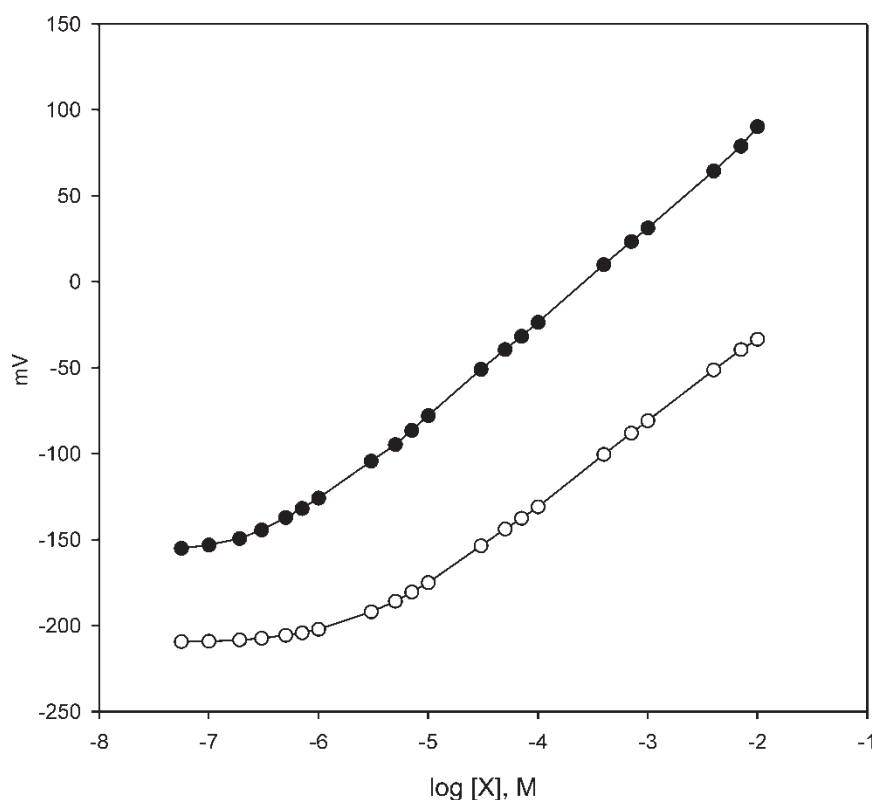|			
Tl—O1	2.864(6)	Tl—O2	2.867(7)
Tl—S2	3.161(2)	Tl—S3	3.2228(17)
O1—Tl—O2	56.96(19)	O1—Tl—S2	62.03(14)
O2—Tl—S2	102.27(19)	O1—Tl—S3	103.25(14)
O2—Tl—S3	61.56(14)	S2—Tl—S3	93.30(5)
S3—C14—C13—O2	57(2)	O2—C12—C11—O1	21(3)
O1—C10—C9—S2	50(2)	O1—C10′—C9—S2	55(2)
S1—C1—C22—S4	59.6(7)		

FIGURE 4 Potentiometric Ag^+ and Tl^+ ion responses of the macrocycle-**2**-based PVC membrane electrodes: (●) $X = Ag^+$; (○) $X = Tl^+$.

Tl^+ ion concentrations, respectively (Fig. 4). Table IV provides the selectivity coefficients of the proposed electrodes for the interfering cations relative to Ag^+ and Tl^+ ions, respectively. For Ag^+ ion, the proposed electrode shows excellent selectivity with respect to the most common metal ions. For example, values of $\log k_{Ag/Y}$ range from -3.6 for K^+ to -4.9 for Ba^{2+} and Ca^{2+}. Indeed responses of less than 10 mV were observed for the divalent cations when their concentrations changed from 0 to 1 mM. In particular, the selectivity coefficient ($\log k_{Ag/Hg}$) for the Hg^{2+} ion, the most severely interfering ion for the electrodes based on sulfur-containing cyclic and acyclic ionophores [4–6], was -4.0. More importantly, in the buffer containing 3 mM sodium cyanide, considerable selectivity towards Tl^+ ($\log k_{Tl/Y}$) was found (Table IV). This is due to the selective blocking of Ag^+ ion by cyanide ion resulting in $Ag(CN)_2^-$. There have been only few reports concerning Tl^+-ISEs [19,20,39–41]. Recently calix[4]arene derivatives have been proposed as Tl^+-ionophores [19,20] followed by Ag^+ ion [42–44] taking advantage of their π-coordination. To our knowledge, this is the first example of a Tl^+ ionophore, the high selectivity of which was explained by the crystal structure, including the π-coordination.

In conclusion, the approach for the development of new types of Tl^+ and Ag^+ ionophore originating

from the crystal structures of the corresponding complexes is reported. Taking this point into account, the X-ray data provided evidence of superior potentiometric sensing with the proposed electrode based on the macrocycle **2**, which can be understood in terms of synergy effects of soft–soft acid–base type and π-coordination, especially for Tl^+ ion.

TABLE IV Potentiometric selectivity coefficients* for the Ag^+ and Tl^+ ion-selective electrodes based on **2**. Y denotes various interfering cations

Cation	$\log k_{Ag/Y}^{pot}$	$\log k_{Tl/Y}^{pot}$
Ag^+	0	-3.1
Tl^+	-0.2	0
Na^+	-3.6	-3.1
K^+	-3.6	-3.1
NH_4^+	-3.6	-3.1
Hg^{2+}	-4.0	-3.7
Co^{2+}	-4.6	-4.2
Pb^{2+}	-4.7	-4.0
Cu^{2+}	-4.7	-4.4
Mg^{2+}	-4.7	-4.5
Cd^{2+}	-4.8	-4.4
Ni^{2+}	-4.8	-4.1
Ba^{2+}	-4.9	-4.3
Ca^{2+}	-4.9	-4.5

*Measured by the separate solution method at 1 mM cation concentration in 0.05 M Tris-nitric acid, pH 9.0; average of three determinations.

References

[1] Izatt, R. M.; Wu, G.; Jiang, W.; Dalley, N. K. *Inorg. Chem.* **1990**, *29*, 3828.
[2] Blake, A. J.; Reid, G.; Schröder, M. *J. Chem. Soc., Chem. Commun.* **1992**, 1074.
[3] Lee, Y. H.; Lee, S. S. *J. Inclusion Phenom.* **2001**, *39*, 235.
[4] Bühlmann, P.; Pretsch, E.; Bakker, E. *Chem. Rev.* **1998**, *98*, 1593.
[5] Casabó, J.; Teixidor, F.; Escriche, L.; Viñas, C.; Pérez-Jiménez, C. *Adv. Mater.* **1995**, *7*, 238, and references cited therein.
[6] Yoon, I.; Lee, Y. H.; Lee, S. S.; Lee, S. C.; Park, S. B. *Analyst* **2001**, *126*, 1773.
[7] Parker, D. In Chapter 3, *Macrocycle Synthesis: A Practical Approach*; Oxford University Press: Oxford, 1996.
[8] Chung, S.; Kim, W.; Kim, D.; Lee, S. S.; Park, S. B. *Talanta* **1997**, *44*, 1291.
[9] Lee, S. S.; Ahn, M.; Park, S. B. *Analyst* **1998**, *123*, 383.
[10] Liu, Y.; Zhang, H.; Chen, L.; He, X.; Wada, T.; Inoue, Y. *J. Org. Chem.* **2000**, *65*, 2870.
[11] Tsukube, H.; Yamada, T.; Shinoda, S. *Ind. Eng. Chem. Res.* **2000**, *39*, 3412.
[12] Ouchi, M.; Hakushi, T. *Coord. Chem. Rev.* **1996**, *148*, 171.
[13] Futterer, T.; Merz, A.; Lex, J. *Angew. Chem., Int. Ed. Engl.* **1997**, *6*, 611.
[14] Dondoni, A.; Ghiglione, C.; Marra, A.; Scoponi, M. *Chem. Commun.* **1997**, 673.
[15] Munakata, M.; Wu, L. P.; Kuroda-Sowa, T.; Maekawa, M.; Suenaga, Y.; Ning, G. L.; Kojima, T. *J. Am. Chem. Soc.* **1998**, *120*, 8610.
[16] Frank, W.; Kuhn, D.; Muller-Becker, S.; Razavi, A. *Angew. Chem., Int. Ed. Engl.* **1993**, *32*, 90.
[17] Kimura, K.; Yajima, S.; Tatsumi, K.; Yojoyama, M.; Oue, M. *Anal. Chem.* **2000**, *72*, 5290.
[18] Choi, B.; Yoon, I.; Kim, J.; Kim, J.; Lee, S. S.; Kim, J. S. *Analyst* **2002**, *127*, 947.
[19] Kimura, K.; Tatsumi, K.; Yokohama, M.; Ouchi, M.; Mocerino, M. *Anal. Commun.* **1999**, *36*, 229.
[20] Park, K. S.; Jung, S. O.; Lee, S. S.; Kim, J. S. *Bull. Korean Chem. Soc.* **2000**, *21*, 909.
[21] Chung, S.; Kim, W.; Park, S. B.; Yoon, I.; Lee, S. S.; Sung, D. D. *Chem. Commun.* **1997**, 965.
[22] Lee, S. S.; Yoon, I.; Park, K.-M.; Jung, J. H.; Lindoy, L. F.; Nezhadali, A.; Rounaghi, G. *J. Chem. Soc., Dalton Trans.* **2002**, 2180.
[23] Livingstone, S. E. *J. Chem. Soc.* **1956**, 437.
[24] Bruker SMART, SAINT, *Version 5.0 (Area Detector Control and Integration Software) and* SHELXTL, *Version 5.16 (Structure Determination Programs)*; Bruker Analytical X-ray Instrument Inc. Madison, WI, 1998.
[25] Sheldrick, G. M. SADABS, *Program for Scaling and Correction of Area Detector Data*; Göttingen University: Germany, 1998.
[26] Schulthess, P.; Ammann, D.; Simon, W.; Caderas, C.; Stepanek, R.; Krautler, B. *Helv. Chim. Acta* **1984**, *67*, 1026.
[27] *Pure Appl. Chem.* **1976**, *48*, 129.
[28] Buter, J.; Kellogg, R. M. *J. Org. Chem.* **1981**, *46*, 4481.
[29] Wolf, R. E. Jr; Hartman, J. R.; Storey, J. M. E.; Foxman, B. M.; Cooper, S. R. *J. Am. Chem. Soc.* **1987**, *109*, 4328.
[30] Zefirov, N. S. *Tetrahedron* **1977**, *33*, 3193.
[31] Wolfe, S. *Acc. Chem. Res.* **1972**, *5*, 102.
[32] Kallert, U.; Mattes, R. *Inorg. Chim. Acta* **1991**, *180*, 263.
[33] Adam, K. R.; Baldwin, D. S.; Duckworth, P. A.; Lindoy, L. F.; McPartlin, M.; Bashall, A.; Powell, H. R.; Tasker, P. A. *J. Chem. Soc., Dalton Trans.* **1995**, 1127.
[34] Park, K.-M.; Yoon, I.; Lee, Y. H.; Lee, S. S. *Inorg. Chim. Acta* **2003**, *343*, 33.
[35] Bondi, A. *J. Phys. Chem.* **1964**, *68*, 441.
[36] Blake, A. J.; Fenske, D.; Li, W.-S.; Lippolis, V.; Schröder, M. *J. Chem. Soc., Dalton Trans.* **1998**, 3961.
[37] Schebler, P. J.; Riordan, C. G.; Guzei, I. A.; Rheingold, A. L. *Inorg. Chem.* **1998**, *37*, 4754.
[38] Galka, C. H.; Gade, L. H. *Inorg. Chem.* **1999**, *38*, 1038.
[39] Tamura, H.; Kimura, K.; Shono, T. *J. Electroanal. Chem.* **1980**, *115*, 115.
[40] Kim, S. M.; Jung, S. O.; Kim, J.; Lee, S. S.; Kim, J. S. *J. Korean Chem. Soc.* **1993**, *37*, 773.
[41] Ouchi, M.; Shibutani, Y.; Yakabe, K.; Shono, T.; Shintani, H.; Yoneda, Y.; Hakushi, T.; Weber, E. *Bioorg. Med. Chem.* **1999**, *7*, 1123.
[42] O'Conner, K. M.; Henderson, W.; O'Neil, E.; Arrigan, D. W. M.; Harris, S. J.; McKervey, M. A.; Svehla, G. *Electroanalysis* **1997**, *9*, 311.
[43] Yaftian, M. R.; Burgard, M.; El Bachiri, A.; Matt, D.; Weiser, C.; Dieleman, C. B. *J. Inclusion Phenom.* **1997**, *29*, 137.
[44] Park, K. S.; Jung, S. O.; Yoon, I.; Park, K.-M.; Kim, J.; Lee, S. S.; Kim, J. S. *J. Inclusion Phenom.* **2001**, *39*, 295.